A Field Study of Whitecap Coverage and its Modulations by Energy Containing Surface Waves

V.A. Dulov, V.N. Kudryavtsev, A.N. Bol'shakov

Marine Hydrophysical Institute (MHI), Sebastopol, Ukraine

A field study of whitecap coverage generated by breaking wind waves has been performed from MHI's Black Sea Research Platform. It is revealed that the main contribution to the whitecap coverage of the sea surface results from breaking of short wind waves, which are more than 3 times shorter than the wavelength of the spectral peak. The energy containing waves strongly modulate the whitecap coverage. Zones of enhanced wave breaking are located on the modulating waves' crests. The effect is described in terms of a modulation transfer function for whitecap coverage. Its magnitude equals about 24, and decreases with the increase of inverse wave age of the energy containing waves.

INTRODUCTION

The breaking of wind waves is one of the most important physical phenomena on the sea surface that results in energy dissipation in wind generated waves, is responsible for turbulent mixing in the sub-surface layer, affects surface drag (supporting air flow separation) and influences air-sea interaction and gas transfer processes. An important application of this study of wave breaking is in the interpretation of radar backscatter from the sea surface, as wave breaking significantly contributes to the radar normalized cross-section.

DESCRIPTION OF THE EXPERIMENT

A field study of wave breaking was performed in October, 1999 from MHI's Research Platform, which is located at a distance of 0.5 km from the Black Sea coast in 30 m of water (Figure 1). The general goals of the experiment were: (i) to understand what spectral range of breaking waves contributes to the total whitecap coverage, and (ii) to analyze the influence of dominant surface waves (waves of the spectral peak and swell) on wave breaking. The latter was treated as a modulation problem.

A view of the platform and plan of the experiment area are shown in Figure 1. Measurements of whitecap coverage were performed by an optical system recording brightness along a 4 meter long linear 'footprint' on the ocean surface. Sampling for brightness of 600 footprint elements was carried out at 10 Hz. The appearance of a whitecap in the footprint was identified if the sea surface brightness exceeded a threshold level. The threshold level was chosen as 3/4 of the averaged (over 3 min.) spikes of brightness. This level automatically follows natural changes in surface illumination (see [*Dulov et al.*, 1998] for details). The optical system footprint was always directed in the main propagation direction of the wave breakers.

The sea surface elevations associated with the wind wave field were registered by four resistance gauges, which formed a spatial grid to assess frequency-directional wave spectra. The footprint of the optical system was located in the vicinity of the wave gauge grid (Figure 1). Wave measurements were accompanied with measurements of wind velocity and air temperature at 19 m height, and seawater temperature.

The experimental conditions are summarized in the Table, where average wind velocity, air and water temperature, significant wave height, frequency of dominant waves and their direction, for each run, are shown.

Gas Transfer at Water Surfaces
Geophysical Monograph 127

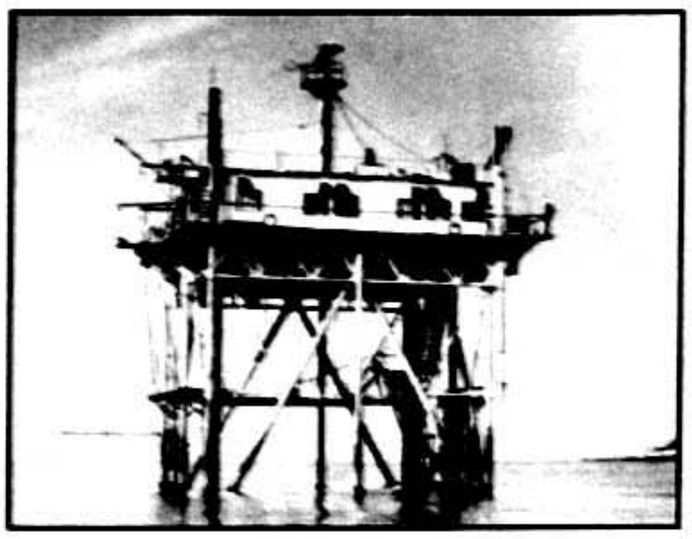

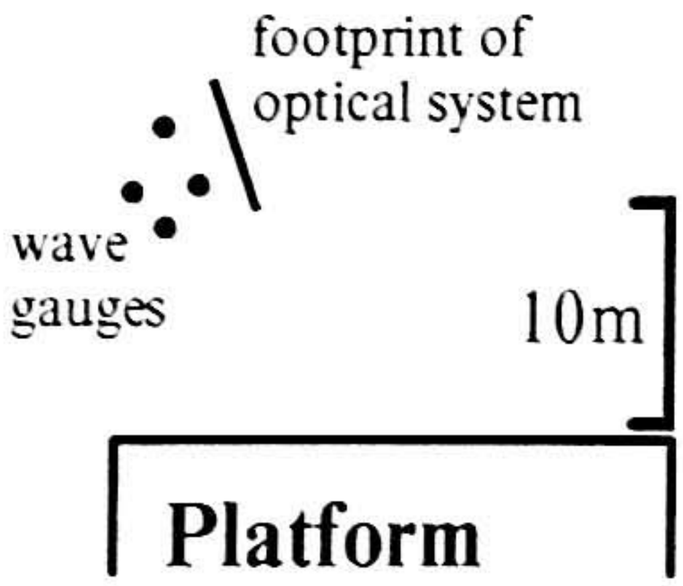

Figure 1. View of the research platform and plan of the layout of the field system.

BACKGROUND CHARACTERISTICS

To analyze the data we have selected two different wind-wave situations. In the first case, the wind-wave field was purely wind generated, and the dominant waves were running along the coast (runs from 4 to 8 in the Table). In the second case, the measurements were done in off-shore wind conditions, when young developing wind waves are running opposite to the swell propagating from the open sea (runs from 1 to 3 in the Table). Examples of the wave frequency spectra for each of these cases are shown in Fig. 2.

A fragment of the spatial-temporal record of the sea surface brightness obtained by the optical system is shown in Figure 3. The vertical axis is distance along the footprint, and the horizontal time-axis is formed by consecutive optical samples. We have used the following procedure of data processing. In those footprint elements where the sea surface brightness exceeds the threshold level, the signal is replaced by 1; in other elements it is replaced by zero. Such a procedure gives explicit mapping for appearance and evolution of individual whitecaps in spatial-temporal images recorded by the optical system (see Figure 3). The number of footprint elements containing ones divided by 600 is treated as an instant fraction of whitecap coverage $q(t)$. This quantity averaged over a certain time gives the mean fraction of the sea surface covered by whitecaps, Q.

In Figure 4 mean values of whitecap coverage Q for all of the runs are shown as a function of wind speed U. The data are consistent with the [*Monahan and Woolf*, 1989] empirical equation for the water-air temperature difference of 7°C, but exhibit a stronger wind exponent. This fact is not surprising, as we have used the data related to both mixed seas and pure wind seas. The other reason is that some of the points were obtained at low wind conditions, when one might expect a steeper wind dependence than is predicted by a cubic relationship.

As is apparent from Figure 3, the spatial-temporal image of the sea surface can be used to assess a speed of whitecap advance along the footprint direction. This speed is equal to the average slope of the whitecap signature in the x-t plane. It can be defined as a slope of a line fitted by least squares to an individual whitecap area. If we contend that the speed of whitecaps can be related to the scale of breaking waves, then a set of whitecaps sorted in accordance with their speed gives us a mechanism by which to determine what spectral range of wind waves contributes to the total whitecap coverage.

We made calculations of the speed C for each individual whitecap and its area in the x-t plane over all the runs. Note

Table. Conditions of the experiments.

	Wind at 19m height:			Dominant waves:			Temperature	
Run	Duration, hours	Speed, m/s	Direction (from)	Significant height, m	Spectral peak frequency, Hz	Direction (from)	Water, °C	Air, °C
1	1.0	10.8	340 °	0.45	0.23	249°	20.5	19
2	0.8	11.1	0 °	0.49	0.21	247°	20.5	19
3	2.3	7.9	328 °	0.36	0.18	204°	19	12.5
4	1.8	5.9	68 °	0.61	0.29	118°	18	11
5	1.4	6.1	58 °	0.64	0.25	113°	18	11
6	1.6	7.9	65 °	1.69	0.16	115°	18	11
7	2.5	7.3	68 °	1.36	0.14	115°	18	11
8	1.5	4.5	60 °	1.08	0.16	108°	18	11

Direction is clockwise relative to the North.

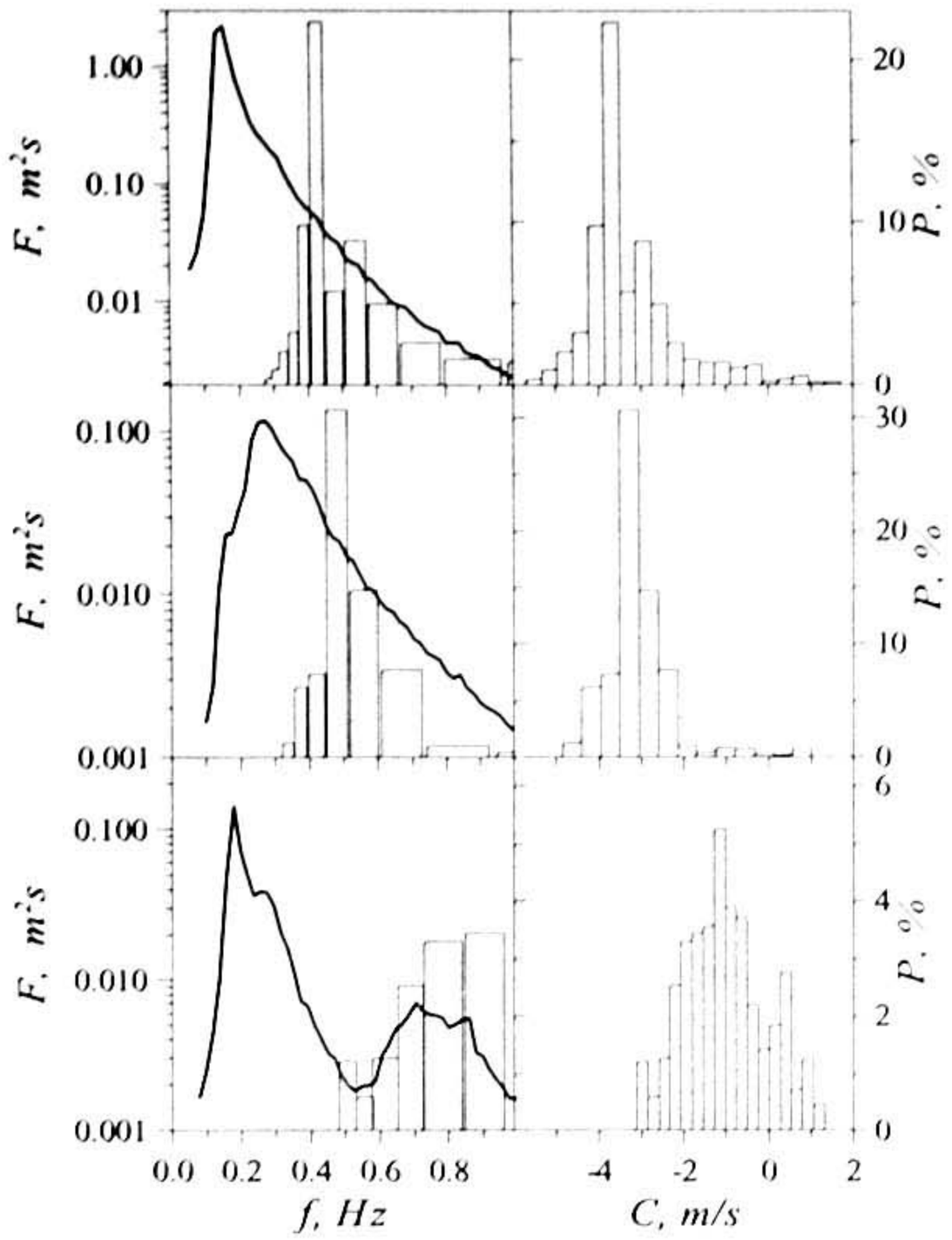

Figure 2. Frequency spectra F (bold line) and contributions in whitecap coverage P (bars) as a function of frequency f and whitecap speed C. The data of two adjacent runs were used for each of plots, the runs shown from the top to the bottom are: 6 and 7; 4 and 5; 1 and 2.

that only those whitecaps were accounted for that consisted of not less than three discrete elements. These data were used to obtain a discrete set Q_j that describes the contribution of whitecaps, which have a velocity of advance in the range from C_j to $C_j+\Delta C_j$, so that the sum of Q_j over all C_j equals the total whitecap coverage Q. Examples of distribution functions

$$P(C_j)= Q_j / Q$$

are shown in the right column of Figure 2.

To relate whitecap speed to a certain scale of breaking waves we assumed following *Phillips* [1985], that C is related to the wave frequency f in accordance with the gravity wave dispersion relation:

$$C = g / (2\pi f)$$

Distribution functions $P(f_j)$ transformed from C to the frequency domain are shown in the left column of Figure 2, along with the wave spectra. The most remarkable conclusion that can be drawn from these plots is that the main contribution of breaking waves to the total whitecap coverage comes not from the dominant waves, but from significantly shorter breaking waves. This fact was reflected in all the data we collected. In cases of pure wind seas (runs from 4 to 8), waves in the wavenumber range $k > 3k_m$ (where k_m is the wavenumber of the spectral peak) contribute more than 90% of the total whitecap coverage. In the case of mixed seas (runs from 1 to 3) wind waves, being the very young waves, support almost the total whitecap coverage.

MODULATIONS OF WAVE BREAKING BY LONG SURFACE WAVES

The fact that breaking of relatively short wind waves is mainly responsible for the total whitecap coverage, results in the question, what is the influence of the energy-containing waves on wave breaking? As a first step we have investigated how dominant surface waves affect spatial distribution of wave breaking.

Whitecaps occur at the sea surface relatively rarely. This means that the temporal variability of the instantaneous values of $q(t)$ measured by our optical system exhibits a noisy signal rather than smooth variations, which could be related to passing dominant waves. That is why to reveal modulation in whitecaps caused by dominant waves, we have used a phase averaging procedure. This procedure has been performed in the following way. As a first step, records of surface elevation have been smoothed to filter out all the surface waves with periods shorter than 2s. Then the smoothed elevations $z(t)$ were split into a number of individual waves. Each individual wave was defined as a tem-

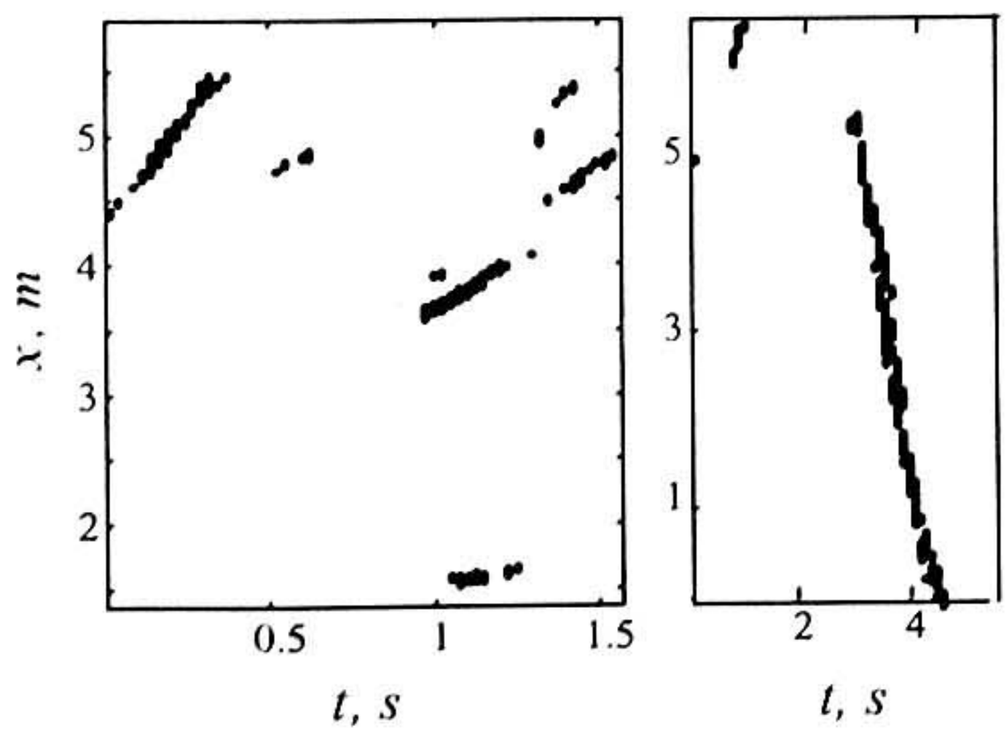

Figure 3. Fragments of the optical record in the time-distance plane. Images of typical whitecaps (left plot) and a large fast whitecap (right plot).

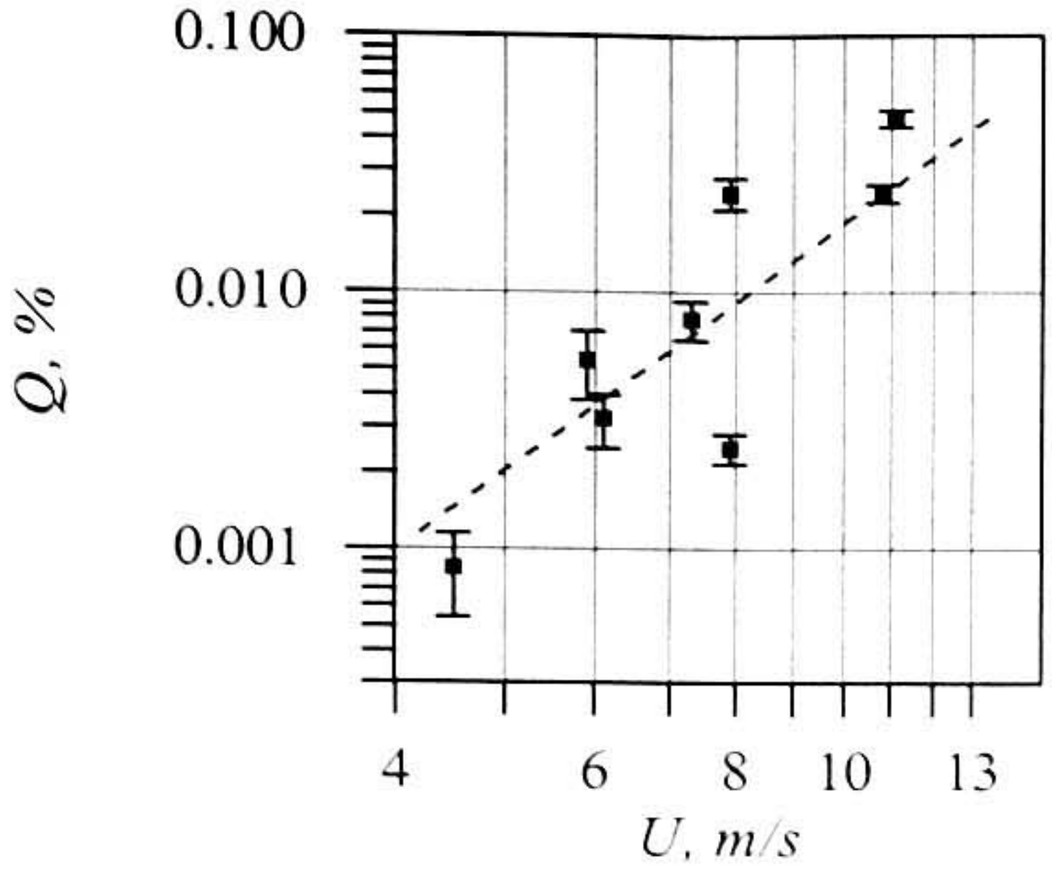

Figure 4. Whitecap coverage percentage as a function of wind speed. Dashed line shows the empirical dependence [by *Monahan and Woolf, 1989*] for water/air temperature difference of 7°C.

poral segment between successive upward zero-crossings of $z(t)$. The length of such temporal segments was treated as a period T_i of individual waves thus defining a wavenumber:

$$K_i = (2\pi / T_i)^2 / g .$$

The surface elevation confined in this interval was considered to be an individual wave profile $z_i(t)$. The series of instantaneous whitecap coverage $q(t)$ has also been split into temporal intervals in accordance with selected individual surface waves, so that each individual wave has been provided with a whitecap coverage fragment $q_i(t)$. Each run consists of 500-1500 individual waves.

As the second step, for each run the set of profiles of individual wave slope $K_i z_i(t)$ and the related set of fragments $q_i(t)$ have been transformed from the temporal domain $0 < t < T_i$ to the phase domain $0 < \tau < 1$, $\tau = t / T_i$ and then have been averaged. Note that only individual waves with frequency less than 0.3-0.4 Hz were taken into account in averaging (as can be seen from Figure 2, this range of dominant waves does not contribute to the whitecap coverage). In the end, we obtained mean profiles of the wave slope $KZ(\tau)$ and corresponding mean distributions of the whitecap coverage $Q(\tau)$ for each run listed in the Table. In Figure 5 some examples of mean slope profiles and distributions of whitecap coverage along them are shown. Vertical bars in Figure 5 show confidence intervals that hereinafter correspond to a single standard error. The remarkable feature is that whitecap coverage is significantly increased on the wave crest and damped in the wave trough vicinity. In cases of pure wind seas (runs 4 to 8), this effect is most pronounced. In the cases when the dominant waves relate to swell (runs from 1 to 3), the effect is also present, but not as evident as in the pure wind sea case.

These data have been analyzed in terms of the modulation transfer function (MTF). The MTF describes the linear response of a sea surface parameter to long surface wave steepness (such quantities are widely used in radar observations, see, e.g. [*Plant*, 1987]). In our case the complex amplitude of the whitecap coverage MTF is defined as

$$M = Q_1 / (Q_0 KA) \qquad (1)$$

where Q_0 is a mean of $Q(\tau)$, Q_1 is a Fourier amplitude of the whitecap coverage variations $Q(\tau)$ along a long wave,

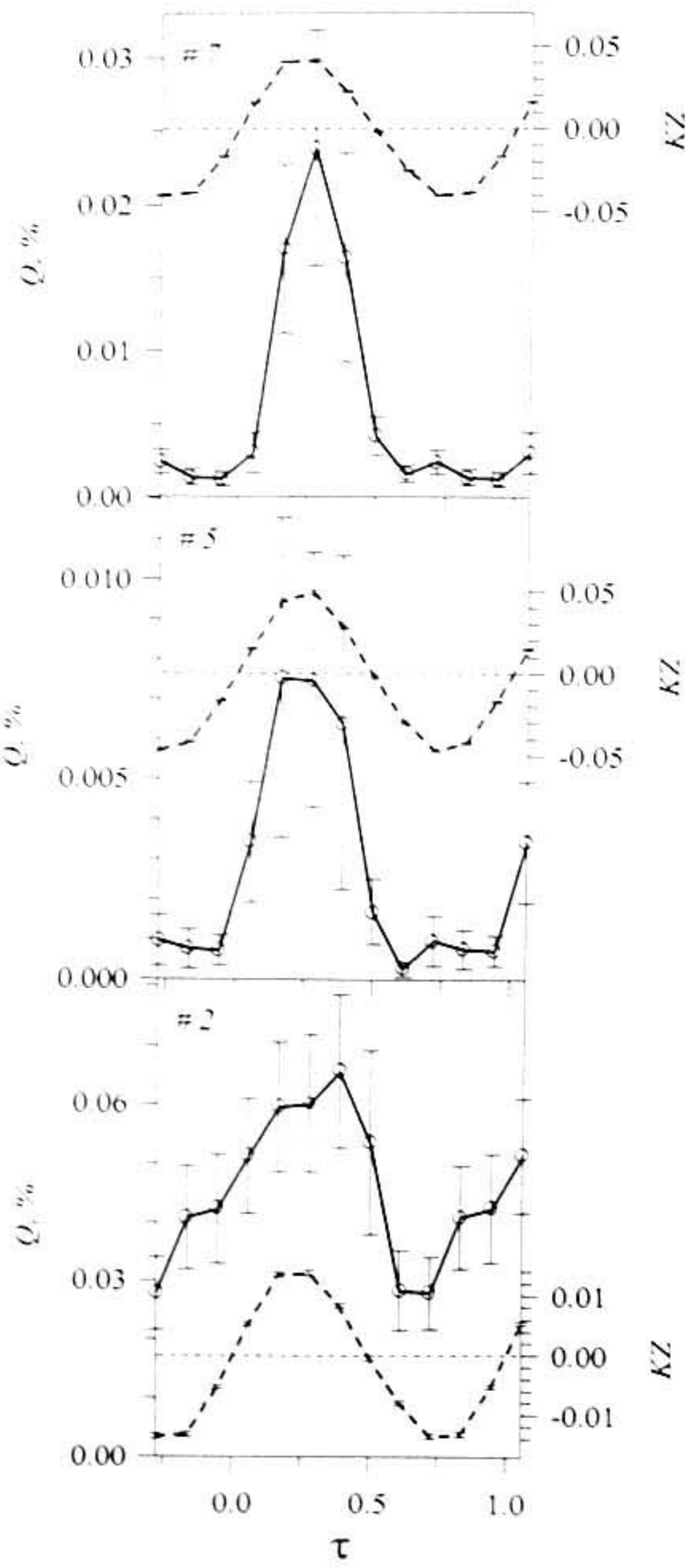

Figure 5. Whitecap coverage distribution Q (solid line with error bars) on a long wave for runs 7, 5 and 2. Dashed line is an elevation profile multiplied by wavenumber, KZ. τ is wave phase divided by 2π.

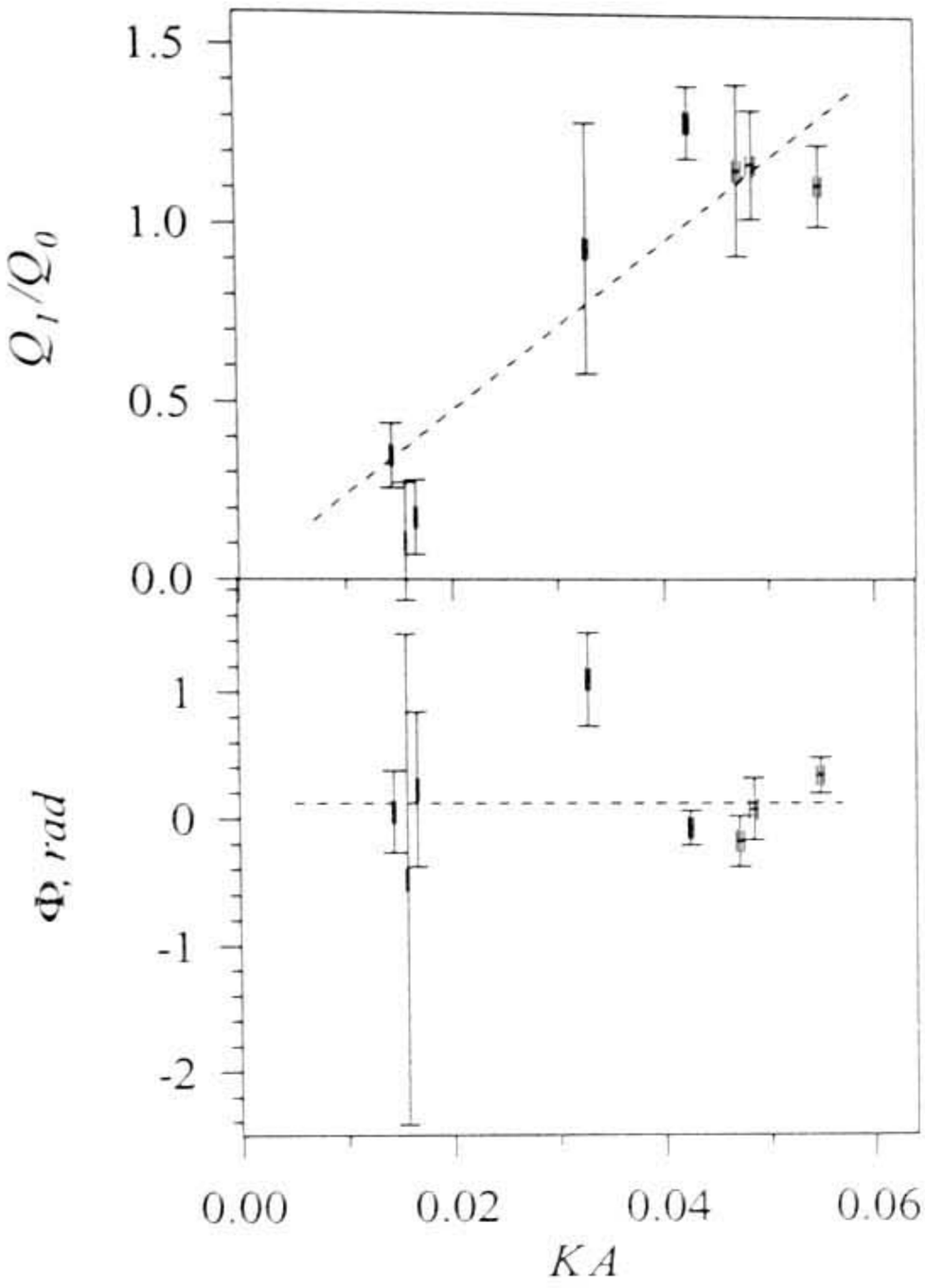

Figure 6. Normalized magnitude Q_1/Q_0 and phase Φ of whitecap modulations as a function of long wave steepness KA. Dashed lines show the estimate (2).

KA is a Fourier amplitude of the profile $KZ(\tau)$ of the long wave steepness. To apply MTF analysis to our data, we have used only the first Fourier harmonics. Dependencies of the magnitude of Q_1 and its phase Φ on KA shown in Figure 6 demonstrate that our data are consistent with equation (1). A least squares estimate of the MTF obtained from these data is

$$|M|=23.8\pm1.3 \qquad \Phi=0.12\pm0.08 \qquad (2)$$

where Φ is in radians. Positive values of the MTF's mean phase show that the zone of enhanced wavebreaking is shifted toward the rear slope of the dominant wave.

The experimental estimates of whitecap coverage MTF were obtained in a relatively wide range of wind-wave conditions (see Table). This makes it possible for us to assess the dependence of $|M|$ on wind speed and frequency of the dominant waves. The latter was used in normalized form, as an inverse wave age, U/C_m, where C_m is phase velocity of the spectral peak. These dependencies are shown in Figure 7. In spite of the scatter, the data exhibit a discernible trend for both wind and age dependencies. As these parameters are correlated for our data, both the trends can be caused by the real MTF dependence on a single parameter. The fact, that the age trend is more clearly expressed in the Figure, advocates the conclusion, that the whitecap MTF decreases with the increase of inverse wave age.

CONCLUSIONS

In this paper we have presented results of an observational study of whitecaps generated by breaking waves and their modulations caused by dominant surface waves. It was revealed that breaking of short wind waves with wavenumbers upwards of 3 times that of the spectral peak are responsible for more than 90% of the whitecap coverage. Contribution of energy-containing waves to whitecap coverage is negligible. The influence of the dominant waves on wave breaking results in very strong modulations in white-capping. Breaking of waves is significantly enhanced at the long wave crests, and is suppressed in the

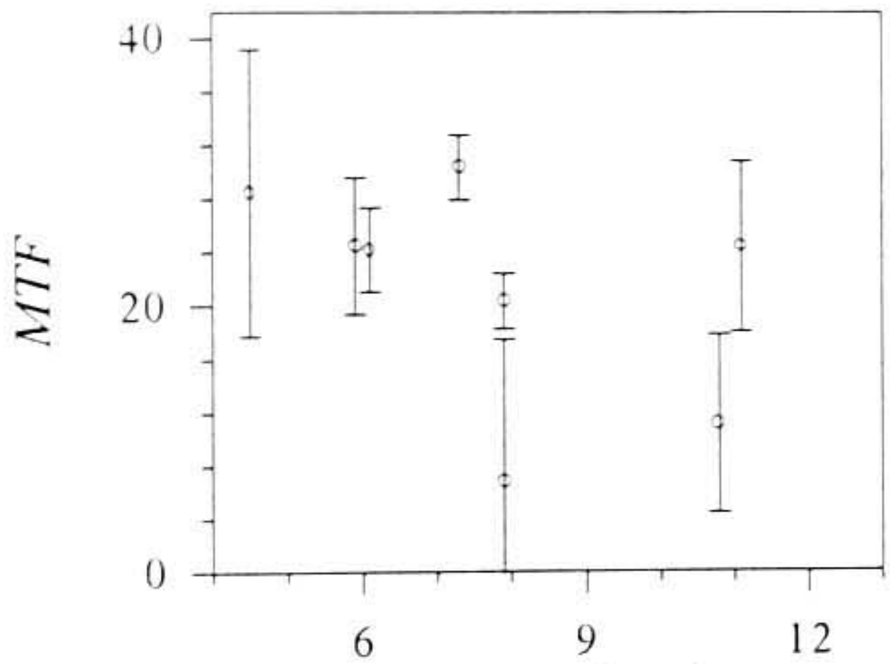

Figure 7. Whitecap MTF as a function of wind speed and inverse wave age.

vicinity of their troughs. The amplitude of whitecap coverage modulations (in terms of the MTF) is approximately equal to 24. This means that the magnitude of the relative variations of whitecap coverage is 24 times larger than the steepness of modulating waves. The whitecap coverage MTF exhibits a dependence on the inverse wave age of the modulating waves: the "older" the dominant waves, the higher the modulations in whitecap coverage.

Acknowledgments. This research was sponsored by the Office of Naval Research (ONR grant N00014-98-10653), and INTAS International Association (grant INTAS/CNES 97-0222).

REFERENCES

Dulov, V.A., Kudryavtsev, V.N., Sherbak, O.G. and Grodsky, S.A. Observations of Wind Wave Breaking in the Gulf Stream Frontal Zone. *The Global Atmosphere and Ocean System*, 1998, Vol. 6, pp.209-242.

Monahan, E.C. and Woolf, D.K. Comments on "Variations of Whitecap Coverage with Wind Stress and Water Temperature". *J. Phys. Oceanogr.*, 1989, Vol. 19, pp. 706-709.

Phillips, O.M. Spectral and statistical properties of the equilibrium range in wind-generated gravity waves. *J. Fluid Mech.*,1985, Vol. 156, pp. 505-531.

Plant, W.J. The Modulation Transfer Function: Concept and Applications. In *Radar Scattering from Modulated Wind Waves*, Eds. G.J. Komen and W.A. Oost, Kluwer Academic Publishers, 1989, pp. 155-172.

Dulov V.A., Kudryavtsev V.N. and Bol'shakov A.N. Marine Hydrophysical Institute, 2 Kapitanskaya str., Sevastopol, Ukraine 99011.
E-mail: odmi@alpha.mhi.iuf.net